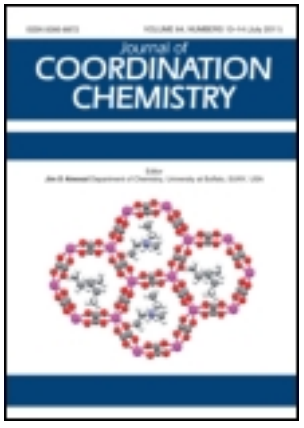

Journal of Coordination Chemistry
Publication details, including instructions for authors and subscription information:
http://www.tandfonline.com/loi/gcoo20

Synthesis, characterization, and DNA damaging of bivalent metal complexes incorporating tetradentate dinitrogen-dioxygen ligand as potential biocidal agents

N. Raman [a], K. Pothiraj [a] & T. Baskaran [a]
[a] Research Department of Chemistry, VHNSN College, Virudhunagar 626 001, Tamil Nadu, India
Published online: 29 Nov 2011.

To cite this article: N. Raman, K. Pothiraj & T. Baskaran (2011) Synthesis, characterization, and DNA damaging of bivalent metal complexes incorporating tetradentate dinitrogen-dioxygen ligand as potential biocidal agents, Journal of Coordination Chemistry, 64:24, 4286-4300, DOI: 10.1080/00958972.2011.638979

To link to this article: http://dx.doi.org/10.1080/00958972.2011.638979

Journal of Coordination Chemistry
Vol. 64, No. 24, 20 December 2011, 4286–4300

Synthesis, characterization, and DNA damaging of bivalent metal complexes incorporating tetradentate dinitrogen–dioxygen ligand as potential biocidal agents

N. RAMAN*, K. POTHIRAJ and T. BASKARAN

Research Department of Chemistry, VHNSN College, Virudhunagar 626 001, Tamil Nadu, India

(*Received 26 August 2011; in final form 26 October 2011*)

A new symmetrical tetradentate Schiff base was prepared by the condensation of 5-nitro-*o*-vanillin and diaminoethane. Its complexes were synthesized and characterized by elemental analysis, magnetic moment, molar conductance, UV-Vis, IR, ^{1}H NMR, ESI-mass, and EPR spectra. The DNA-binding behavior of these complexes was investigated by absorption spectra, cyclic voltammetry, and viscosity measurements. The DNA-binding constants for Co(II), Ni(II), Cu(II), and Zn(II) complexes were 1.58×10^4, 1.65×10^4, 2.71×10^4, and 1.83×10^4 $(\text{mol L}^{-1})^{-1}$, respectively. The results suggest that the complexes intercalate between DNA base pairs. Further, all these complexes exhibit moderate to high ability to cleave pUC19 DNA. The ligand and its complexes have been screened for antimicrobial activities using the disc diffusion method against selected bacteria and fungi. Antibacterial activity was greater against Gram-positive than Gram-negative bacteria for Cu(II) complex and antifungal activity was greater against *Aspergillus niger* and *Candida albicans* for the Cu(II) complex.

Keywords: Schiff base; Metal complexes; EPR spectra; DNA binding; DNA damage

1. Introduction

Schiff bases are used extensively as ligands in coordination chemistry [1, 2]. Chelating ligands containing O and N donors show broad biological activity and are of special interest because of the variety of ways in which they bond to metal ions. Recent years have witnessed great interest in synthesis and characterization of transition metal complexes containing Schiff bases due to their application as catalysts for many reactions [3], their relationship to synthetic and natural oxygen carriers, and also their use as new structural probes in nucleic acid chemistry and as therapeutic agents [4]. There is a considerable interest in Schiff bases and their complexes for their striking anticancer, antibacterial, antiviral, antifungal, and other biological properties [5, 6].

There has been increasing focus on binding of small molecules to DNA [7, 8]. Errors in gene expression can often cause diseases and play a secondary role in the outcome and severity of human diseases [9]. A more complete understanding of DNA-drug

*Corresponding author. Email: drn_raman@yahoo.co.in

ISSN 0095-8972 print/ISSN 1029-0389 online
http://dx.doi.org/10.1080/00958972.2011.638979

binding is valuable in the design of DNA structural probes, DNA foot printing, sequence-specific cleaving agents, and potential anti-cancer drugs [10, 11].

In order to develop new drugs which specifically target DNA, it is necessary to understand the different binding modes of small molecules. Non-covalent binding of small molecules to DNA are intercalative, groove, and external electrostatic binding [12, 13]. Among these interactions, intercalation and groove binding are the most important DNA-binding modes as they invariably lead to cellular degradation. Metal ion type and different functional groups of ligands, which are responsible for the geometry of complexes, also affect the affinity of metal complexes to DNA [14–16]. Investigation on the interaction of Schiff-base transition metal complexes with DNA has significance for disease defense, new medicine design, and clinical application of drugs.

Herein, our interest in the synthesis and structural characterization of a new Schiff base and its metal complexes involve desired biological activity to establish spectroscopic bioactive model complexes. Since a few unsymmetrical 5-nitro-*o*-vanillin-diamine Schiff-base compounds have been reported, this article deals with the synthesis and spectroscopic characterization of metal(II) complexes with symmetrical Schiff-base ligand derived from 5-nitro-*o*-vanillin and diaminoethane [17]. The free ligand and its complexes have been tested for *in vitro* microbial properties against *Staphylococcus aureus*, *Bacillus subtilis*, *Escherichia coli*, *Pseudomonas aeruginosa*, *Aspergillus niger*, *Rhizopus stolonifer*, *Candida albicans*, and *Rhizoctonia bataicola* by using the disc diffusion method.

2. Experimental protocols

2.1. *Materials and physical measurements*

All reagents and chemicals were of reagent grade quality, and 5-nitro-*o*-vanillin and diaminoethane were obtained from Sigma Aldrich (Bangalore, India). Analytical reagent grade $CoCl_2 \cdot 6H_2O$, $NiCl_2 \cdot 6H_2O$, $CuCl_2 \cdot 2H_2O$, and $ZnCl_2$ were used. Calf-thymus (CT-DNA) and Tris-HCl buffer were purchased from Himedia, Bangalore, India. The plasmid supercoiled (SC) pUC19 DNA was purchased from Bangalore Genei, Bangalore, India. Agarose (molecular biology grade) and ethidium bromide (EB) were obtained from Sigma Aldrich (St. Louis, USA). Tris-HCl buffer was prepared using deionized and sonicated triply-distilled water. Solvents used for electrochemical and spectral measurements were purified by the reported procedures [18].

Carbon, hydrogen, and nitrogen analyses of the ligand and its complexes were carried out on a CHN analyzer Carlo Erba 1108, Heraeus, Texas city, USA. Infrared spectra (4000–400 cm^{-1} KBr disks) of the samples were recorded on an Affinity-1 FT-IR spectrophotometer. Electronic absorbance spectra of the ligand and its complexes in DMF solution (200–1100 nm) were recorded on a UV-1601 spectrophotometer (Shimadzu, Tokyo, Japan). ^1H NMR spectra of ligand and its nickel and zinc complexes (300 MHz) were recorded on a Bruker Avance DRX-300 FT-NMR spectrometer using DMSO-d_6 as solvent. Tetramethylsilane was used as internal standard. Chemical shifts were reported in δ scale. EPR spectra of complexes in solid

state at 300 K and in frozen DMSO at 77 K were recorded on a Varian E–112 spectrometer at X-band, using TCNE as marker with 100 kHz modulation frequency and 9.5 GHz microwave frequency. Mass spectrometry experiments were performed on a JEOL-AccuTOF JMS-T100LC mass spectrometer equipped with a custom-made electrospray interface (ESI). Molar conductance of 10^{-3} mol L^{-1} solution of the complexes in *N*,*N*′-dimethyl formamide (DMF) were measured at room temperature with an Deep Vision Model-601 digital direct reading deluxe conductivity meter. Magnetic susceptibility measurements were carried out by employing the Gouy method at room temperature on powder sample of the complex. $CuSO_4 \cdot 5H_2O$ was used as calibrant. The metal contents of the complexes were determined according to the literature method [19].

2.2. *Biological studies*

2.2.1. UV-Vis spectroscopy. All experiments involving interaction of the complexes with DNA were carried out in Tris-HCl buffer (5 mmol L^{-1} Tris-HCl/50 mmol L^{-1} NaCl buffer, pH 7.2). A solution of DNA in the buffer gave a ratio of UV absorbance at 260 and 280 nm of about 1.8–1.9, indicating that the DNA was sufficiently free of protein [20]. The DNA concentration per nucleotide was determined by absorption spectroscopy using the molar absorption coefficient (6600 (mol L^{-1})$^{-1}$ cm^{-1}) at 260 nm. Absorption titration experiments were performed by maintaining the metal complex concentration as constant at 10 μmol L^{-1} while varying the concentration of the CT-DNA within 5–40 μmol L^{-1}. While measuring the absorption spectra, equal quantity of CT-DNA was added to both the complex and the reference solution to eliminate the absorbance of DNA itself.

2.2.2. Electrochemical studies. Cyclic voltammetry was carried out at CH instrument electrochemical analyzer. All voltammetric experiments were performed in single compartmental cell of volume 10–15 mL containing a three electrode system comprised of a glassy carbon working electrode, platinum wire as counter electrode, and a Ag/AgCl electrode as reference electrode. The supporting electrolyte was 5 mmol L^{-1} Tris-HCl/50 mmol L^{-1} NaCl buffer (pH 7.2) in deionized water. Deaerated solutions were used by purging N_2 gas for 15 min prior to measurements.

2.2.3. Determination of viscosity. Viscosity experiments were conducted on an Ubbelodhe viscometer, immersed in a thermostatic water-bath maintained to 30°C. Titrations were performed for the investigated complexes (2–16 μmol L^{-1}), and each complex was introduced into a DNA solution (20 μmol L^{-1}) present in the viscometer. Data are presented as $(\eta/\eta_0)^{1/3}$ *versus* the ratio of the concentration of the complex and DNA (R), where η is the viscosity of DNA in the presence of the complex and η_0 is the viscosity of DNA alone. Relative viscosities for DNA in either the presence or absence of investigated complexes were calculated from the following equation [21]:

$$\eta = (t - t_0)/t_0$$

where t is the observed flow time of the DNA containing solution and t_0 is the flow time of Tris-HCl buffer solution.

2.2.4. DNA cleavage studies. The cleavage of DNA was monitored using agarose gel electrophoresis. Supercoiled pUC19 DNA (0.2 μg) in Tris-HCl buffer (5 mmol L^{-1} Tris-HCl/50 mmol L^{-1} NaCl buffer, pH 7.2) was treated with metal complexes (25 μmol L^{-1} and 50 μmol L^{-1}) and hydrogen peroxide (2 μL, 100 μmol L^{-1}) followed by dilution with Tris-HCl buffer to a total volume of 20 μL. The samples were incubated for 1 h at 37°C. A loading buffer containing 25% bromophenol blue, 0.25% xylene cyanol and 30% glycerol were added and electrophoresis was performed at 50 V for 3 h in TBE buffer using 0.8% agarose gel containing 1.0 μg mL^{-1} ethidium bromide. Bands were visualized using UV light and photographed. The cleavage mechanism was investigated by using the hydroxyl radical scavenger (DMSO, ethanol, and *t*-BuOH), the singlet oxygen scavengers (L-histidine and NaN_3), and the superoxide anion radical scavenger superoxide dismutase (SOD). All experiments were carried out in triplicate under the same conditions.

2.2.5. Determination of microbial analysis. The *in vitro* antimicrobial screening effects of the synthesized ligand and its metal complexes were evaluated against four species of bacteria (*S. aureus*, *B. subtilis*, *E. Coli*, and *P. aeruginosa*) as well as fungi (*A. niger*, *R. stolonifer*, *C. albicans*, and *R. bataicola*) by disc diffusion method [22, 23]. All the tests were performed in triplicate and average is reported. The minimum inhibitory concentration (MIC) values of the studied compounds against tested microorganisms were also reported. Schiff-base ligand, metal complexes, ciprofloxacin, and fluconazole were dissolved in DMSO at 100 μg mL^{-1}. The two-fold dilutions of the solution were prepared (0.78–100 μg mL^{-1}). The microorganism suspensions at 10^6 CFU mL^{-1} (colony forming unit mL^{-1}) concentrations were inoculated to the corresponding wells. The plates were incubated at 37°C for 24 and 48 h for the bacteria and fungi, respectively. The MIC values were determined as the lowest concentration that completely inhibited visible growth of the microorganism as detected by unaided eye.

2.3. *Inorganic compound preparation*

2.3.1. Preparation of Schiff base (H_2L). The tetradentate Schiff base was synthesized by the following method. An ethanol solution (20 mL) containing diaminoethane (0.601 g, 10 mmol) was added to an ethanol solution (50 mL) containing 5-nitro-*o*-vanillin (3.942 g, 20 mmol). The mixture was stirred for 3 h and an orange red precipitate was separated. The precipitate was filtrated and washed with ethanol and then dried in air.

2.3.2. Preparation of metal complexes. Hot ethanolic solution (25 mL) of the Schiff base (0.418 g, 1.0 mmol) was added to a solution of cobalt(II) chloride hexahydrate (0.237 g, 1.0 mmol), nickel(II) chloride hexahydrate (0.237 g, 1.0 mmol), copper(II)

chloride dihydrate (0.170 g, 1.0 mmol), or zinc(II) chloride (0.136 g, 1.0 mmol) in the same solvent (15 mL). The solution was then refluxed for 2 h, cooled, and evaporated at room temperature. The precipitated complexes that separated were filtered, washed with ether, and dried in vacuum over anhydrous calcium chloride.

3. Results and discussion

Analytical data of the ligand and its metal complexes are in agreement with those required by the general formula $[MC_{18}H_{16}N_4O_8]$ (where M = cobalt(II), nickel(II), copper(II), and zinc(II)) (table S1, Supplementary material). The obtained complexes are insoluble in water, methanol, ethanol, and chloroform but soluble in DMF and DMSO.

3.1. *Molar conductance measurements*

By using the relation $\Lambda_M = K/C$, the molar conductances of the prepared complexes at 10^{-3} mol L^{-1} DMF were in the range of 23.82–26.65 $Ohm^{-1}cm^2mol^{-1}$ (table S2, Supplementary material). These values indicate that the synthesized complexes are non-electrolytes, in accord with conductivity values for non-electrolytes below 50 $Ohm^{-1}cm^2mol^{-1}$ in DMF solution [24].

3.2. *Electronic spectra and magnetic moment*

The electronic spectrum of the ligand shows peaks at 325, 280, and 235 nm, assigned to $n \rightarrow \pi^*$ of −CH=N and $\pi \rightarrow \pi^*$ aromatic ring, respectively [25]. On complexation, these peaks are shifted to higher wavelengths suggesting coordination of azomethine nitrogen and phenolic oxygen. From table S2, the electronic spectrum of the Ni(II) complex showed an absorption band at 501 nm for $^1A_{1g} \rightarrow {}^1A_{2g}$ of a four-coordinate, square-planar geometry. The electronic spectrum of Cu(II) complex showed bands at 528 and 441 nm assignable to $^2B_{1g} \rightarrow {}^2A_{1g}$ and $^2B_{1g} \rightarrow {}^2E_g$ transitions, respectively, which correspond to square-planar Cu(II) [26]. The electronic spectrum of Co(II) complex showed a broad band at 540 nm, assigned to the $^4A_2(F) \rightarrow {}^4T_1(P)$ transition, suggesting tetrahedral geometry around Co(II). Since the zinc ion has d^{10} configuration, the absorption at 340 nm could be assigned to a charge transfer transition. However, taking into account the spectrum and the configuration of zinc(II), tetrahedral geometry could be assumed for its complex [27].

The nickel(II) complex was diamagnetic due to square-planar geometry around the Ni(II). The magnetic moment for copper(II) complex is 1.84 B.M. at 300 K, consistent with expected spin-only magnetic moment of $S = 1/2$, d^9 copper(II) demonstrating that the complex was monomeric with the absence of metal–metal interaction. The magnetic moment of the Co(II) complex was 3.85 B.M., close to the spin-only magnetic moments ($\mu_{eff} = 3.87$ B.M.) for three unpaired electrons [28].

Table 1. IR stretching frequency data of ligand and its metal(II) complexes (ν (cm^{-1})).

Compound	–OH	Ar–CH	Aliphatic-CH	–CH=N	Ar–C=C	$–NO_2$	–C–O	M–O	M–N
HL	3335	3078	2970, 2937	1622	1545	1523	1230	–	–
[CoL]	–	3079	2970, 2934	1605	1541	1522	1285	525	433
[NiL]	–	3078	2971, 2936	1609	1542	1523	1280	522	440
[CuL]	–	3080	2972, 2935	1610	1543	1521	1272	513	437
[ZnL]	–	3081	2972, 2934	1607	1544	1520	1278	519	435

3.3. *Infrared spectra*

In order to study the coordination of the Schiff base to the metal ions, IR spectrum of the free Schiff base is compared with spectra of the complexes (table 1). The IR spectrum of H_2L has a broad band at 3335 cm^{-1} assigned to ν(OH). The disappearance of this band in spectra of the complexes indicates deprotonation of hydroxyl and coordination through deprotonated phenolic OH [29]. In the free ligand, the high-intensity band due to ν(C–O) (aromatic carbon and phenolic oxygen) at 1230 cm^{-1} [30] appeared as a medium intensity band at 1272–1285 cm^{-1}, indicating coordination of the phenolic oxygen to metal [31] and formation of M–O bond *via* deprotonation. However, the strong band at 1622 cm^{-1} in the free Schiff base is assigned to azomethine vibration. This band shifts to lower frequencies by 10–17 cm^{-1} in the complexes, indicating coordination of the imine nitrogen to metal [32]. The band at 1520–1523 cm^{-1} in the free ligand as well as the complexes is assigned to stretching vibration of $\upsilon(NO_2)$. Two new bands at 513–525 and 433–440 cm^{-1} are assigned to ν(M–O) and ν(M–N) [33], respectively, supporting the participation of nitrogen of the azomethine and oxygen of OH of the ligand in complexation with metal, as shown in scheme 1.

3.4. *^{1}H NMR spectra*

The ^{1}H NMR spectra of the ligand, nickel(II), and zinc(II) complexes are taken in DMSO-d_6 and the chemical shift data are given in table 2. The phenolic OH signal at 11.50 ppm in the spectrum of the ligand is not seen in spectra of the Ni(II) and Zn(II) complexes, indicating the participation of phenolic OH in chelation with proton displacement. The signal due to azomethine proton shifts upon complexation, probably due to donation of the lone pair of electrons on nitrogen to the central metal, resulting in the formation of a coordinate linkage ($M \rightarrow N$). The aromatic protons resonate as a multiplet at 7.20–7.85 ppm. The signal due to methoxy attached to the aromatic ring is observed at almost the same chemical shift as in the spectrum of H_2L.

3.5. *Mass spectra*

The electron impact mass spectra provide a vital character for interpretation of the structure of the free tetradentate Schiff-base ligand and its copper(II) complex, for example. The mass spectrum of H_2L is given in figure S1 (Supplementary material). The spectrum shows the molecular ion peak M^+ at m/z 418, which is matched with the

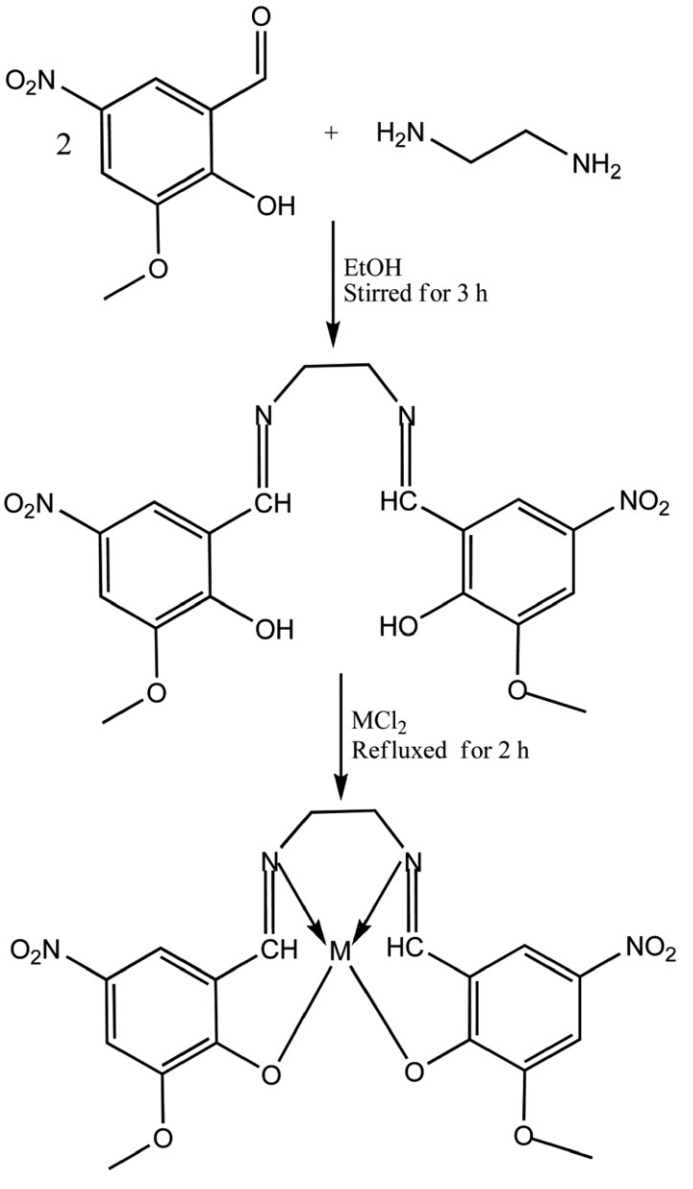

Scheme 1. Preparation of Schiff base and its metal(II) complexes.

Table 2. ^{1}H NMR chemical shift data of ligand and its nickel(II) and zinc(II) complexes (δ (ppm)).

Compound	Phenolic-OH	–CH=N	Ar–H	–OCH_3	–CH_2
HL	11.50	9.16	7.20–7.82	3.74	2.36
[NiL]	–	8.87	7.21–7.83	3.76	2.39
[ZnL]	–	8.83	7.22–7.85	3.75	2.38

suggested structure as well as the molecular weight. The ESI-mass spectra of Ni(II) and Cu(II) complexes show molecular ion peaks M^+ at m/z 476 and 481, respectively, equivalent to their molecular weights. Ni(II) and Cu(II) complexes undergo demetallation to form the fragment ion $[C_{18}H_{16}N_4O_8]^+$, which is observed at m/z 416. In addition to this, the fragment ions $[C_8H_6N_2O_4]^+$, $[C_7H_5NO_4]^+$, and $[C_6H_2NO_4]^+$ are observed at m/z 194, 167, and 153, respectively. All these fragmentation peaks were observed in the ESI-mass spectra in Ni(II) and Cu(II) complexes. This spectral evidence reveals that the formed complexes have equimolar ratio of metal salts and ligand, as prescribed in scheme 1.

3.6. *EPR spectra of Cu(II) complex*

The X-band EPR spectra of copper complex in DMSO at 300 and 77 K are shown in figures S2 and S3, respectively, and discussed in the "Supplementary material."

3.7. *DNA binding characteristics of metal complexes*

3.7.1. Effect of CT-DNA on absorption spectra. Electronic absorption spectroscopic titration is an effective method to examine the binding of DNA with metal complexes since the observed changes of spectra may give evidence of the interaction [34]. In general, hyperchromism and hypsochromism are spectral features of DNA concerning changes of its double helix structure, hyperchromism means breaking the secondary structure of DNA, and hypsochromism shows that binding of complex to DNA can be due to electrostatic effect or intercalation which may stabilize the DNA duplex. Additionally, the existence of a blue-shift is indicative of the stabilization of DNA duplex [35]. In order to quantitatively compare binding strength of the complexes, the intrinsic binding constants K_b of the complexes with DNA were calculated using the following equation [36]:

$$[DNA]/(\varepsilon_a - \varepsilon_f) = [DNA]/(\varepsilon_b - \varepsilon_f) + 1/K_b(\varepsilon_b - \varepsilon_f)$$

where [DNA] is the concentration of DNA in base pairs, the apparent absorption coefficient ε_a, ε_f, and ε_b correspond to A_{obsd}/[complex], the extinction coefficient for the free metal complex, for each addition of DNA to the metal complex and metal complex in the fully bound form, respectively. In plots $[DNA]/(\varepsilon_a - \varepsilon_f)$ *versus* [DNA], K_b is given by the ratio of slope to y intercept. Fixed amounts (10 μmol L^{-1}) of complexes were titrated with increasing amounts of DNA. The electronic spectral trace of copper complex is given in figure 1. For complexes, the absorption spectra clearly show that the addition of DNA to the complexes yields hyperchromism and a blue shift to the ratio of [DNA]/[complex]. Obviously, these spectral characteristics suggest that all the complexes interact with DNA most likely through a mode that involves stacking interaction between the aromatic chromophore and the base pairs of DNA. Addition of increasing amounts of DNA resulted in hypsochromism of the peak maxima in the UV-Vis spectra of the complexes. The binding constants for metal(II) complexes vary from 1.58×10^4 to 2.71×10^4 $(\text{mol L}^{-1})^{-1}$ (table 3). The DNA-binding constant of the complexes are comparable to those of some DNA intercalative polypyridyl ruthenium(II) complexes ($1.0–4.8 \times 10^4$ $(\text{mol L}^{-1})^{-1}$) [37].

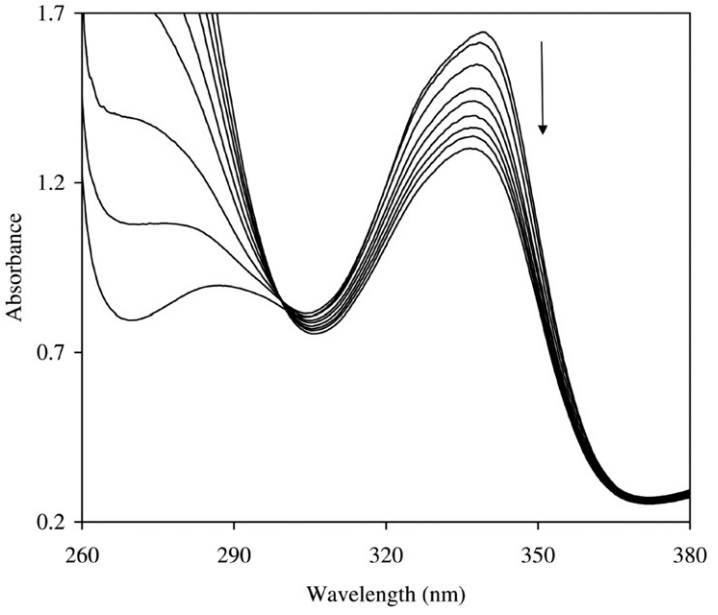

Figure 1. Absorption spectrum of copper(II) complex in the absence and presence of increasing amounts of CT-DNA at room temperature in 5 mmol L^{-1} Tris-HCl/50 mmol L^{-1} NaCl buffer (pH 7.2). Arrow shows the absorbance change upon increasing the DNA concentration.

Table 3. Electronic absorption properties of metal(II) complexes with CT-DNA.

	λ_{max} (nm)				
Complex	Free	Bound	$\Delta\lambda$ (nm)	Hypochromicity (%)	$K_b \times 10^4$ $((\text{mol L}^{-1})^{-1})$
[CoL]	337.6	336.3	1.3	13.54	1.58
[NiL]	338.0	336.6	1.4	15.43	1.65
[CuL]	338.2	336.0	2.2	20.68	2.7
[ZnL]	339.5	337.8	1.7	17.22	1.83

3.7.2. Effect of CT-DNA on cyclic voltammetry. The application of electrochemical methods to study of metallointercalation and coordination of transition metal complexes to DNA provides a useful complement to electronic absorption spectroscopy [38, 39]. Typical cyclic voltammetry (CV) behavior of Cu(II) complex in the absence and presence of CT-DNA is shown in figure 2. The CV of the Cu(II) complex in the absence of DNA featured two anodic peaks ($E^1_{pa} = 0.136$ V and $E^2_{pa} = -0.247$ V *vs.* Ag/AgCl) and two cathodic peaks ($E^1_{pc} = 0.070$ V and $E^2_{pc} = -0.784$ V *vs.* Ag/AgCl). The oxidation peak potentials E^1_{pa} and E^2_{pa} belong to Cu(I)/Cu(II) and Cu(0)/Cu(I) and the corresponding reduction of Cu(II) and Cu(I) occurred upon scan reversal at 0.070 V and −0.247 V, respectively. The separation of the anodic and cathodic peak potentials (ΔE_p) for Cu(II)/Cu(I) and Cu(I)/Cu(0) couple is 0.066 and 0.537 V, respectively. The ratio of anodic to cathodic peak currents (I_{pa}/I_{pc}) is nearly one for Cu(II)/Cu(I) couple,

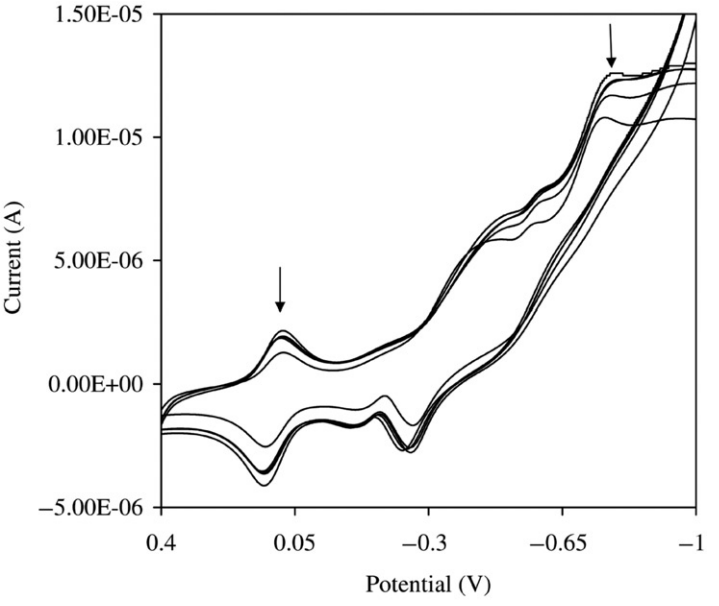

Figure 2. Cyclic voltammogram of copper(II) complex in the absence and presence of increasing amounts of CT-DNA at room temperature in DMSO : buffer (1 : 2) mixture (pH 7.2). Arrow shows the current change upon increasing the DNA concentration.

Table 4. Electrochemical behavior of metal(II) complexes in the absence and presence of CT-DNA.

		E_{pc} (V)		E_{pa} (V)		ΔE_p (V)		$E_{1/2}$ (V)	
Complex	Redox couple	Free	Bound	Free	Bound	Free	Bound	Free	Bound
[NiL]	Ni(II)/Ni(I)	−0.584	−0.573	−0.329	−0.316	0.255	0.257	−0.456	−0.444
[CuL]	Cu(II)/Cu(I)	0.070	0.077	0.136	0.142	0.066	0.065	0.103	0.109
	Cu(I)/Cu(0)	−0.784	−0.766	−0.247	−0.232	0.537	0.534	−0.515	−0.499
[CoL]	Co(I)/Co(0)	−0.898	−0.888	–	–	–	–	–	–
[ZnL]	Zn(II)/Zn(I)	−0.770	−0.753	–	–	–	–	–	–

indicating a reversible redox process, whereas the (I_{pa}/I_{pc}) value is less than one for Cu(I)/Cu(0) redox couple for quasi-reversible process. The formal potential $E_{1/2}$, taken as average of E_{pc} and E_{pa} for Cu(II)/Cu(I) and Cu(I)/Cu(0) couple is 0.103 and −0.515 V, respectively, in the absence of DNA. The presence of DNA in solution at the same concentration of Cu(II) complex causes a slight decrease in the voltammetric current coupled with a slight shift in the peak potential to more positive. The decrease of the voltammetric currents and the shift of the peak potential in the presence of CT-DNA can be attributed to diffusion of the metal complex bound to the large, slowly diffusing DNA. The CV of the Ni(II) complex in 1 : 2 DMSO : buffer solution, the potentials (E_{pc}(f) and E_{pa}(f)) for the quasi-reversible redox couple Ni(II)/Ni(I) have been determined and their values are given in table 4. The changes of the redox couple Ni(II)/Ni(I) upon the addition of CT-DNA have been studied and the potentials (E_{pc}(b)

and E_{pa}(b)) as well as the corresponding shifts (ΔE_p and $E_{1/2}$) are given in table 4. In the absence of CT-DNA, the CV of Co(II) and Zn(II) complexes only show the cathodic reduction peak potential. The addition of different concentrations of CT-DNA to cobalt and zinc complexes, the shifts in the voltammetric current, and peak potentials show that the complexes bind to DNA on the electrode surface and their cathodic peak potential values are given in table 4. In general, the electrochemical potential of a small molecule will shift positively when it intercalates into the DNA double helix and shifts in a negative direction for electrostatic interaction with DNA. When more than one potential exists, a positive shift of E_p^1 and negative shift of E_p^2 imply that the molecule binds to DNA by both intercalation and electrostatic interaction [40]. No new redox peaks appeared after the addition of CT-DNA to each complex, but the current of all the peaks decreased significantly, suggesting the existence of interaction between each complex and CT-DNA. The decrease in current can be explained as an equilibrium mixture of free and DNA-bound complex to the electrode surface. For increasing amounts of CT-DNA, shifts in the cathodic (E_{pc}) and anodic (E_{pa}) potentials of all four complexes shows a positive shift ($\Delta E_{pc}^1 = +0.007$ V, $\Delta E_{pa}^1 = +0.006$ V, $\Delta E_{pc}^2 = +0.018$ V and $\Delta E_{pa}^2 = +0.015$ V for Cu(II) complex, $\Delta E_{pc} = +0.011$ V and $\Delta E_{pa} = +0.013$ V for Ni(II) complex, $\Delta E_{pc} = +0.010$ V for Co(II) complex and $\Delta E_{pc} = +0.017$ V for Zn(II) complex), suggesting an intercalative mode of binding.

3.7.3. Effect of CT-DNA on viscosity measurements. Intercalation results in a lengthening of DNA, thus producing increases in relative specific viscosity of solutions of DNA [20]. To probe the nature of the interaction between metal complexes and DNA, the effect of the addition of metal complexes on the viscosity of aqueous CT-DNA solutions was studied. Figure S4 (Supplementary material) shows the changes in the relative viscosity of CT-DNA on the addition of complexes. Increasing amounts of complexes increased the relative viscosity of CT-DNA solution steadily, confirming that these complexes interact with CT-DNA through intercalation.

3.8. *DNA damaging of metal complexes*

In DNA damaging studies, DNA binding is the main biological event that triggers anticancer properties of the metal complexes. Studies on the interaction between the transition metal complexes and DNA are important to further understand their pharmacology. Since DNA is an important cellular receptor, many compounds exert their antitumor effects through binding to DNA, thereby changing the replication of DNA and inhibiting the growth of tumor cells, which is the basis for designing new and more efficient antitumor drugs. Their effectiveness depends on the mode and affinity of the binding [41, 42]. DNA cleavage is controlled by relaxation of the supercoiled circular conformation of pUC19 DNA leading to nicked circular and/or linear conformations. When electrophoresis is applied to circular plasmid DNA, the fastest migration will be observed for DNA of closed circular conformations (Form I). If one strand is cleaved, the supercoil will relax and produce a slower moving nicked conformation (Form II). If both strands are cleaved, a linear conformation (Form III) will appear between Forms I and II. In order to determine the ability of complexes for DNA scission, the complexes were incubated with supercoiled pUC19 DNA for 1 h in Tris-HCl buffer (5 mmol L^{-1} Tris-HCl/50 mmol L^{-1} NaCl buffer, pH 7.2) at two

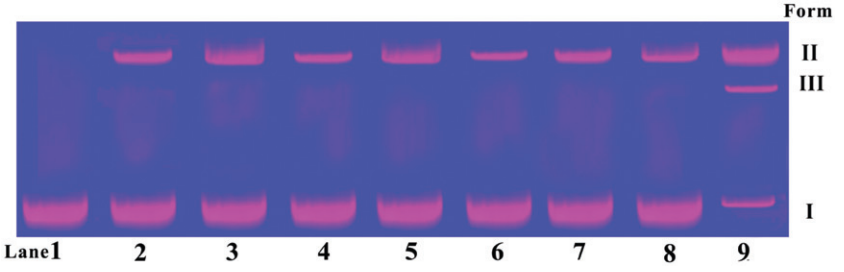

Figure 3. Gel electrophoresis diagram showing the cleavage of supercoiled pUC19 DNA (0.2 μg) in 5 mmol L^{-1} Tris-HCl/50 mmol L^{-1} NaCl buffer (pH 7.2) incubated at 37°C for 1 h with two different concentrations of complexes in the presence of H_2O_2 Lane 1, Control DNA; Lane 2, DNA + H_2O_2 (100 μmol L^{-1}) + [ZnL] (25 μmol L^{-1}); Lane 3, DNA + H_2O_2 (100 μmol L^{-1}) + [ZnL] (50 μmol L^{-1}); Lane 4, DNA + H_2O_2 (100 μmol L^{-1}) + [NiL] (25 μmol L^{-1}); Lane 5, DNA + H_2O_2 (100 μmol L^{-1}) + [NiL] (50 μmol L^{-1}); Lane 6, DNA + H_2O_2 (100 μmol L^{-1}) + [CoL] (25 μmol L^{-1}); Lane 7, DNA + H_2O_2 (100 μmol L^{-1}) + [CoL] (50 μmol L^{-1}); Lane 8, DNA + H_2O_2 (100 μmol L^{-1}) + [CuL] (25 μmol L^{-1}); Lane 9, DNA + H_2O_2 (100 μmol L^{-1}) + [CuL] (50 μmol L^{-1}), respectively.

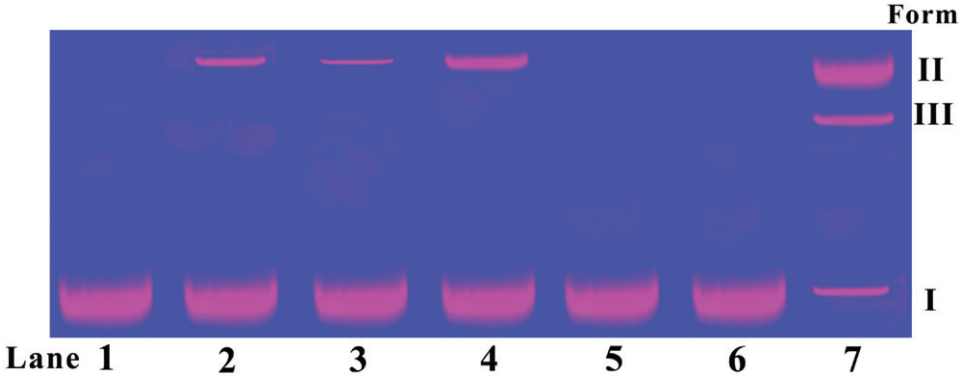

Figure 4. Gel electrophoresis diagram showing the cleavage of supercoiled pUC19 DNA (0.2 μg) by [CuL] (50 μmol L^{-1}) with the addition of H_2O_2 (100 μmol L^{-1}) and radical scavengers in 5 mmol L^{-1} Tris-HCl/ 50 mmol L^{-1} NaCl buffer (pH 7.2) and incubated at 37°C for 1 h: Lane 1, DNA control; Lanes 2–7, DNA + H_2O_2 + [CuL] (50 μmol L^{-1}) + radical scavengers (DMSO (4 μL), ethanol (4 μL), *t*-BuOH (100 μmol L^{-1}), L-histidine (100 μmol L^{-1}), NaN_3 (100 μmol L^{-1}) and SOD (4 units), respectively).

different concentrations using hydrogen peroxide; the DNA cleavage activities of the Co(II), Ni(II), Cu(II), and Zn(II) complexes were studied by gel electrophoresis using supercoiled pUC19 DNA (0.2 μg) in Tris-HCl buffer. Control experiments do not show cleavage of DNA (figure 3, lane 1). As shown in figure 3, when the complex concentration increases, the intensity of the circular supercoiled DNA (Form I) decreases and that of the nicked (Form II) increases. All the complexes exhibit nuclease activity. At 25 μmol L^{-1} (figure 3, lanes 2, 4, 6, and 8), Zn(II), Ni(II), Co(II), and Cu(II) complexes show minimal cleavage activity whereas at 50 μmol L^{-1} (figure 3, lanes 3, 5, 7, and 9) they show moderate to higher cleavage activity. Under the same experimental conditions, Cu(II) complex exhibit more effective DNA cleavage activity than the other three complexes. The different cleaving efficiencies may be ascribed to different binding affinity of the four metal complexes to DNA.

Table 5. The *in vitro* antimicrobial activity of ligand and its metal(II) complexes evaluated by MIC ($\mu g\,mL^{-1}$).

	Antibacterial activity				Antifungal activity			
Complex	*S. aureus*	*B. subtilis*	*E. coli*	*P. aeruginosa*	*A. niger*	*R. bataicola*	*R. stolonifer*	*C. albicans*
H_2L	25	50	50	100	50	50	100	25
[CoL]	6.25	6.25	6.25	25	6.25	12.50	25	3.125
[NiL]	3.125	6.25	12.50	25	6.25	6.25	12.50	3.125
[CuL]	0.78	1.56	3.125	6.25	0.78	3.125	6.25	1.56
[ZnL]	3.125	3.125	6.25	12.50	3.125	6.25	12.50	6.25
Ciprofloxacin	0.78	1.56	0.78	1.56	–	–	–	–
Flucanozole	–	–	–	–	0.78	1.56	1.56	1.56

Involvement of reactive oxygen species (hydroxyl radical, superoxide ion, singlet oxygen) in nuclease activity could be diagnosed by monitoring the quenching of DNA cleavage in the presence of radical scavengers in solution. Hydroxyl radical scavengers like DMSO, ethanol, and *t*-BuOH showed partial inhibition of nuclease activity (figure 4, lanes 2–4). These results suggest that hydroxyl radicals may be involved in the cleavage process. Addition of singlet oxygen scavengers like l-histidine and NaN_3 (lanes 5 and 6) showed complete inhibition of nuclease, suggesting that $^1O_2$ or any other singlet oxygen-like entity may participate in the DNA strand scission. SOD addition (lane 7) does not have any apparent effect on the cleavage activity, indicating non-involvement of superoxide radical in the cleavage reaction. This implied that DNA cleavage by the complex should be realized by an oxidative cleavage pathway.

3.9. *Antimicrobial assay*

To assess biological potential of the synthesized ligand and its metal complexes, they were tested against different species of bacteria and fungi. The results of the antimicrobial activity of the synthesized compounds (MIC value) are given in table 5 and discussed in the "Supplementary material."

4. Conclusion

This work reports the synthesis, characterization, and electronic absorption spectra of tetradentate Schiff base (H_2L) and its transition metal complexes [CoL], [NiL], [CuL], and [ZnL]. The synthetic procedure in this work results in the formation of $1:1\,M:H_2L$ complexes. The metal(II) ions are coordinated by two phenolic oxygens and two azomethine nitrogens (–CH=N) of the ligand with square-planar geometry around Cu(II) and Ni(II) complexes and tetrahedral geometry around Co(II) and Zn(II) complexes. DNA-binding study indicates that intrinsic binding constant of complexes from 1.58×10^4 to 2.71×10^4 $(mol\,L^{-1})^{-1}$ is comparable to those of some DNA

intercalative complexes (1.0×10^4–4.8×10^4 $(\text{mol L}^{-1})^{-1}$). The complexes bind to DNA by classical intercalation. The mechanism for DNA cleavage by the complex is oxidative cleavage. The antimicrobial screening of ligand and its synthesized metal complexes, particularly copper complex, displayed promising antibacterial and fungal activity compared to known antibiotic drugs. Detailed studies on these results and related complexes and the biological applications are in progress.

Acknowledgments

The authors express their heartfelt thanks to the College Managing Board, Principal, and Head of the Department of Chemistry, VHNSN College, for providing necessary research facilities. Instrumental facilities provided by Sophisticated Analytical Instrumental Facility (SAIF), IIT Bombay, and CDRI, Lucknow, are gratefully acknowledged.

References

[1] A.A.A. Emara. *Spectrochim. Acta, Part A*, **77**, 117 (2010).
[2] W.-Y. Bi, X.-Q. Lü, W.-L. Chai, J.-R. Song, W.-Y. Wong, W.-K. Wong, R.A. Jones. *J. Mol. Struct.*, **891**, 450 (2008).
[3] H. Zhang, S. Xiang, J. Xiao, C. Li. *J. Mol. Catal. A: Chem.*, **238**, 175 (2005).
[4] S. Delaney, M. Pascaly, P.K. Bhattacharya, K. Han, J.K. Barton. *Inorg. Chem.*, **41**, 1966 (2002).
[5] K. Ghosh, P. Kumar, N. Tyagi, U.P. Singh, N. Goel. *Inorg. Chem. Commun.*, **14**, 489 (2011).
[6] V. Mishra, S.N. Pandeya, S. Anathan. *Acta Pharm. Turc.*, **2**, 139 (2000).
[7] K.E. Erkkila, D.T. Odom, J.K. Barton. *Chem. Rev.*, **9**, 2777 (1999).
[8] A. Chouai, S.E. Wicke, C. Turro, J. Bacsa, K.R. Dunbar, D. Wang, R.P. Thummel. *Inorg. Chem.*, **4**, 5996 (2005).
[9] J. Hooda, D. Bednarski, L. Irish, S.M. Firestine. *Bioorg. Med. Chem.*, **4**, 1902 (2006).
[10] F. Liang, P. Wang, X. Zhou, T. Li, Z.Y. Li, H.K. Lin, D.Z. Gao, C.Y. Zheng, C.T. Wu. *Bioorg. Med. Chem. Lett.*, **14**, 1901 (2004).
[11] P. Krishnamoorthy, P. Sathyadevi, A.H. Cowley, R.R. Butorac, N. Dharmaraj. *Eur. J. Med. Chem.*, **46**, 3376 (2011).
[12] G.M. Zhang, S.M. Shuang, C. Dong, D.S. Liu, M.F. Choi. *J. Photochem. Photobiol. B*, **74**, 127 (2004).
[13] S. Sharma, S.K. Singh, M. Chandra, D.S. Pandey. *J. Inorg. Biochem.*, **99**, 458 (2005).
[14] L. Wang, Y. Zhu, Z. Yang, J. Wu, Q. Wang. *Polyhedron*, **10**, 2477 (1991).
[15] I.-ul-H. Bhat, S. Tabassum. *Spectrochim. Acta, Part A*, **72**, 1026 (2009).
[16] V. Uma, M. Kanthimathi, T. Weyhermuller, B.U. Nair. *J. Inorg. Biochem.*, **99**, 2299 (2005).
[17] E.J. Campbell, S.T. Nguyen. *Tetrahedron Lett.*, **42**, 1221 (2001).
[18] D.X. West, A.A. Nasar. *Transition Met. Chem.*, **24**, 617 (1999).
[19] R.J. Angellici. *Synthesis and Techniques in Inorganic Chemistry*, W.B. Saunders Company, Philadelphia, PA (1969).
[20] S. Satyanaryana, J.C. Dabrowial, J.B. Chaires. *Biochemistry*, **31**, 9319 (1992).
[21] M. Eriksson, M. Leijon, C. Hiort, B. Norden, A. Graeslund. *Biochemistry*, **33**, 5031 (1994).
[22] A.W. Bauer, W.W.M. Kirby, J.C. Sherris, M. Turck. *Am. J. Clin. Pathol.*, **45**, 493 (1966).
[23] M.S.A. El-Gaby. *Chinese Chem. Soc.*, **51**, 125 (2004).
[24] W.J. Geary. *Coord. Chem. Rev.*, **7**, 81 (1971).
[25] D.N. Sathyanarayana. *Electronic Absorption Spectroscopy and Related Techniques*, Universities Press (India) Limited, Hyderabad, India (2001).
[26] M. Shakir, A. Abbasia, A.U. Khan, S.N. Khan. *Spectrochim. Acta, Part A*, **78**, 29 (2011).
[27] S.M.E. Khalil, H.F.O. El-Shafiy. *Synth. React. Inorg. Met.-Org. Chem.*, **30**, 1817 (2000).
[28] E. Tas, A. Kilic, N. Konak, I. Yilmaz. *Poyhedron*, **27**, 1024 (2008).
[29] N. Shahabadi, S. Kashanian, F. Darabi. *Eur. J. Med. Chem.*, **45**, 4239 (2010).
[30] S. Sarkar, K. Dey. *Spectrochhim. Acta A*, **62**, 383 (2005).

[31] A. Saxena, J.P. Tandon. *Polyhedron*, **3**, 681 (1984).
[32] G.B. Bagihalli, P.G. Avaji, S.A. Patil, P.S. Badami. *Eur. J. Med. Chem.*, **43**, 2639 (2008).
[33] K. Nakamoto. *Infrared Raman Spectra of Inorganic and Coordination Compounds*, 3rd Edn, John Wiley and Sons, New York (1992).
[34] H. Chao, W. Mei, Q. Huang, L. Ji. *J. Inorg. Biochem.*, **92**, 165 (2002).
[35] M. Patel, M. Chhasatia, P. Parmar. *Eur. J. Med. Chem.*, **45**, 439 (2010).
[36] A. Wolfe, G.H. Shimer, T. Meehan. *Biochemistry*, **2620**, 6392 (1897).
[37] X.W. Liu, J. Li, H. Deng, K.C. Zheng, Z.W. Mao, L.N. Ji. *Inorg. Chim. Acta*, **358**, 3311 (2005).
[38] N. Raman, A. Selvan. *J. Coord. Chem.*, **64**, 534 (2011).
[39] M.T. Carter, D.R. Bard. *J. Am. Chem. Soc.*, **109**, 7528 (1987).
[40] S.S. Zhang, S.Y. Niu, B. Qu, G.F. Jie, H. Xu, C.F. Ding. *J. Inorg. Biochem.*, **99**, 2340 (2005).
[41] Y.W. Jung, S. Lippard. *J. Chem. Rev.*, **107**, 1387 (2007).
[42] A. Dedieu. *Chem. Rev.*, **100**, 543 (2000).